Fast Transient Currents in Na,K-ATPase Induced by ATP Concentration Jumps from the P^3-[1-(3′,5′-Dimethoxyphenyl)-2-Phenyl-2-Oxo]ethyl Ester of ATP

Valerij S. Sokolov,*# Hans-Jürgen Apell,* John E. T. Corrie,§ and David R. Trentham§

*Department of Biology, University of Konstanz, Konstanz, Germany; #A. N. Frumkin Institute of Electrochemistry, Academy of Sciences of Russia, Moscow, Russia; and §National Institute for Medical Research, Mill Hill, London NW7 1AA, England

ABSTRACT Electrogenic ion transport by Na,K-ATPase was investigated by analysis of transient currents in a model system of protein-containing membrane fragments adsorbed to planar lipid bilayers. Sodium transport was triggered by ATP concentration jumps in which ATP was released from an inactive precursor by an intense near-UV light flash. The method has been used previously with the P^3-1-(2-nitrophenyl)ethyl ester of ATP (NPE-caged ATP), from which the relatively slow rate of ATP release limits analysis of processes in the pump mechanism controlled by rate constants greater than 100 s^{-1} at physiological pH. Here Na,K-ATPase was reinvestigated using the P^3-[1-(3,5-dimethoxyphenyl)-2-phenyl-2-oxo]ethyl ester of ATP (DMB-caged ATP), which has an ATP release rate of $>10^5$ s^{-1}. Under otherwise identical conditions, photorelease of ATP from DMB-caged ATP showed faster kinetics of the transient current compared to that from NPE-caged ATP. With DMB-caged ATP, transient currents had rate profiles that were relatively insensitive to pH and the concentration of caged compound. Rate constants of ATP binding and of the E_1 to E_2 conformational change were compatible with earlier studies. Rate constants of enzyme phosphorylation and ADP-dependent dephosphorylation were 600 s^{-1} and 1.5×10^6 M^{-1} s^{-1}, respectively, at pH 7.2 and 22°C.

INTRODUCTION

Na,K-ATPase in the plasma membrane of animal cells carries out uphill transport of sodium and potassium ions at the expense of free energy of ATP hydrolysis (Glynn, 1985; Läuger, 1991). The stoichiometry of three Na^+/2 K^+ ions transported per ATP hydrolyzed leads to movement across the membrane of one net charge per cycle. This indicates the existence of one or more electrogenic reaction steps. In recent publications it has been shown that the major charge-translocating steps occur in the sodium-transporting branch of the pump cycle (Nakao and Gadsby, 1986; Borlinghaus et al., 1987; Heyse et al., 1994; Sagar and Rakowski, 1994; Hilgemann, 1994; Wuddel and Apell, 1995). In the reaction sequence of Na^+ translocation,

$$E_1 \rightleftharpoons Na_2E_1 \rightleftharpoons Na_3E_1 \rightleftharpoons Na_3E_1ATP$$

$$\rightleftharpoons (Na_3)E_1\text{-}P \rightleftharpoons P\text{-}E_2(Na_3) \rightleftharpoons P\text{-}E_2$$

several nonzero dielectric coefficients have been obtained: 1) for the binding of the third Na^+ ion, $Na_2E_1 \rightleftharpoons Na_3E_1$ ($\alpha = 0.25$); 2) for the conformational transition, $(Na_3)E_1$-P $\rightleftharpoons$ P-$E_2(Na_3)$ ($\beta = 0.1$); 3) for the release of the first Na^+ ion on the extracellular side, P-$E_2(Na_3) \rightleftharpoons$ P-$E_2(Na_2)$ ($\delta_0 = 0.65$); and 4) for the subsequent release of the second and third ions, P-$E_2(Na_2) \rightleftharpoons$ P-E_2 ($\delta_1 = \delta_2 = 0.1$). The Greek letters represent the dielectric coefficients, which characterize the contribution of the corresponding reaction step to the current movement (Läuger and Apell, 1986; Läuger, 1991). The meaning of the brackets in the reaction sequence is described in the legend to Fig. 1. The above Na^+ translocation sequence forms a component of a complete Na,K-ATPase cycle in the absence of K^+ (the "Na-only" mode; Fig. 1), which has been modeled to describe the pump mechanism with rate constants and other parameters listed in Table 1 (Wuddel and Apell, 1995).

A variety of methods have been applied to analyze the kinetics of the Na^+ translocation and to determine the kinetic constants of this partial reaction. Nakao and Gadsby (1986) used the whole-cell clamp technique to measure the voltage dependence of the rate-limiting reaction step. In this electrophysiological method, the pump current was obtained as the cardiac-glycoside-dependent component of the total current. A recent development in this method is the giant-patch technique, which allowed a significantly higher time resolution (Hilgemann, 1994; Lu et al., 1995; Friedrich et al., 1996). Another method is an optical approach using fluorescent styryl dyes (such as RH421) to detect changes in the local electric field in pump-containing membranes produced by electrogenic reactions (Klodos and Forbush, 1988; Forbush and Klodos, 1991; Stürmer et al., 1991; Heyse et al., 1994).

A different approach to direct electric measurements is to analyze charge movements in purified membrane fragments that contain a high concentration of Na,K-ATPase and are capacitively coupled to planar lipid bilayers (Fendler et al., 1985; Borlinghaus et al., 1987; Wuddel and Apell, 1995). In these experiments the pump activity is triggered by an ATP concentration jump produced by photolytic release of ATP from an inactive precursor called caged ATP. The electrogenic steps of the Na,K-ATPase reaction sequence generate

Received for publication 21 April 1997 and in final form 23 January 1998.

Address reprint requests to Dr. Hans-Jürgen Apell, University of Konstanz, Fach M 635, D-78457 Konstanz, Germany. Tel.: 011-49-7531-88-2253; Fax: 011-49-7531-88-3183; E-mail: h-j.apell@uni-konstanz.de.

0006-3495/98/05/2285/14 $2.00

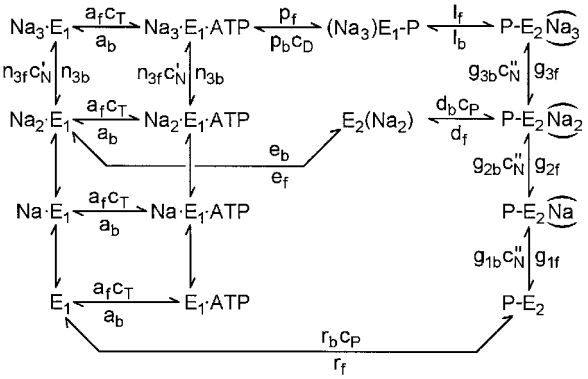

FIGURE 1 Kinetic reaction cycles of Na^+ transport in Na,K-ATPase ("Na-only mode") according to Wuddel and Apell (1995). a_f, p_f, . . . and a_b, p_b, . . . are the rate constants in the forward and backward directions, respectively. c_T, c_D, and c_P represent the concentrations of ATP, ADP, and P_i. c'_N and c''_N are the sodium concentrations on the cytoplasmic and extracellular sides of the membrane. Transitions between E_1, Na_2E_1, and Na_3E_1 and between E_1ATP, Na_2E_1ATP, and Na_3E_1ATP were assumed to be fast compared to the other reaction steps with equilibrium constants K_1 and K_{n3} respectively. In states $(Na_3)E_1$-P and $E_2(Na_2)$, the ions are occluded, i.e., they cannot exchange with either aqueous phase. The horizontally placed brackets in the P-E_2 states are used in this reaction scheme to indicate that the ion binding sites are situated inside an ion well (Läuger, 1991). These horizontal brackets are drawn vertically in the text.

a transient current that can be analyzed in terms of a reaction cycle as shown in Fig. 1 (Borlinghaus and Apell, 1988; Wuddel and Apell, 1995). Thus rapid release of ATP initiates a sequence of transitions between the discrete states, E_1, Na_2E_1, . . . P-E_2, which are controlled by the forward and backward rate constants shown in Fig. 1. For example, the net rate Φ_{n3} of the transition $Na_2E_1 \rightleftharpoons Na_3E_1$ is given by $\Phi_{n3} = n_{3f}[Na^+][Na_2E_1] - n_{3b}[Na_3E_1]$. Defining corresponding rates for all transitions and their corresponding dielectric coefficients, α_i, the pump current $I_p(t)$ is represented by

$$I_p(t) = e_o N \sum_i \alpha_i \Phi_i(t)$$

where e_o is the elementary charge and N is the number of pump molecules in the membrane (Apell et al., 1987; Wuddel and Apell, 1995).

Thus in terms of Fig. 1 and the data in Table 1, rapid release of ATP from caged ATP in the presence of Na,K-ATPase and Na^+ (i.e., starting from Na_3E_1) would generate a high concentration of $(Na_3)E_1$-P nonelectrogenically, and thus transformation of $(Na_3)E_1$-P to P-$E_2(Na_3)$. . . . P-E_2, which involves electrogenic steps, would be reflected in a high $I_p(t)$ that decayed at $\sim$25 s^{-1} (i.e., limited by rate constant l_f) to a steady-state intermediate of P-$E_2(Na_x)$, where $x = 0$, 1, 2 or 3. In more general terms, a high value of $I_p(t)$ is compatible with the rapid build-up of intermediate state(s) through a series of nonelectrogenic steps and then transformation by a rate-limiting process through one or more electrogenic steps. It is also noteworthy that the rate of current decay, here measured in the absence of K^+ and at room temperature, is approximately equal to the k_{cat} of Na,K-ATPase when measured under optimized conditions of ATP, Mg^{2+}, Na^+, and K^+, because K^+ promotes rapid dephosphorylation of P-E_2 (Heyse et al., 1994).

Previous transient current studies have used the P^3-1-(2-nitrophenyl)ethyl ester of ATP (NPE-caged ATP), for which the kinetics of ATP release upon photolysis are dependent on pH, Mg^{2+} concentration, and ionic strength (Walker et al., 1988; McCray and Trentham, 1989). The rate constant for ATP release at pH 7.1, 21°C, and ionic strength 0.18 M in the presence of 3 mM Mg^{2+} is 86 s^{-1} (Walker et al., 1988), significantly slower than p_f, the rate constant controlling phosphorylation (i.e., $Na_3E_1ATP \rightarrow (Na_3)E_1$-P), which has been estimated to be in the range of 200–500 s^{-1} (Heyse et al., 1994; Keillor and Jencks, 1996). In addition, binding of NPE-caged ATP to the nucleotide binding site (Forbush, 1984a; Nagel et al., 1987; Borlinghaus and Apell, 1988) had to be taken into account in the kinetic analyses. Therefore, in the transient current experiments referred to above, the phosphorylation kinetics and the photorelease of ATP had to be deconvoluted, and the results of the analysis were inaccurate, especially in determining p_f.

To overcome this difficulty, we have used the P^3-[1-(3′,5′-dimethoxyphenyl)-2-phenyl-2-oxo]ethyl ester of ATP (DMB-caged ATP) (Thirlwell et al., 1994), which releases ATP on photolysis at a rate greater than 10^5 s^{-1}, which is not detectably affected by changes in pH or Mg^{2+} concentration (Corrie et al., 1992). Thus it should be possible to determine rate constants a_f and p_f (Table 1) from the transient currents without interference from slow release of ATP on caged ATP photolysis. Furthermore, the influence of ADP on the transient currents using DMB-caged ATP should permit estimates of p_b.

An abstract reporting some of this work has been published (Sokolov et al., 1997).

MATERIALS AND METHODS

Materials

L-1,2-Diphytanoyl-3-phosphatidylcholine was obtained from Avanti Polar Lipids (Birmingham, AL); sodium dodecyl sulfate (SDS) was from Pierce Chemical (Rockford, IL). Phosphoenolpyruvate, pyruvate kinase, lactate dehydrogenase, NADH, ATP (disodium salt, special quality), and the ATP Bioluminescence Assay Kit HS II were from Boehringer (Mannheim). Apyrase VI was purchased from Sigma (Munich), and the P^3-1-(2-nitrophenyl)ethyl ester of ATP (NPE-caged ATP) was from Molecular Probes (Eugene, OR). NaCl (suprapure quality) and all other reagents (at least analytical grade) were from Merck (Darmstadt).

Preparation and photochemistry of DMB-caged ATP

DMB-caged ATP (potassium salt) was synthesized as described (Thirlwell et al., 1994). Spontaneous hydrolysis of DMB-caged ATP, releasing ADP and DMB-caged phosphate, occurs at a rate of 2.4×10^{-4} h^{-1} at pH 7 and 30°C (Thirlwell et al., 1994), and, as prepared, DMB-caged ATP was contaminated with $\sim$1% ADP (mol/mol). ADP was removed as necessary by apyrase (see below). The photolysis by-product, 5,7-dimethoxy-2-phe-

TABLE 1 Kinetic and dielectric parameters of the electrogenic reaction steps in the Na-only mode of Na,K-ATPase

Reaction	Parameter	Equilibrium constant	Value in forward direction	Dielectric coefficient	Ref.[§]
$E_1 \rightleftharpoons Na_2E_1$		$K_1 = 3$ mM	*	0	1
$Na_2E_1 \rightleftharpoons Na_3E_1$	n_3	$K_{n3} = 4$ mM	$2 \times 10^4\ M^{-1}s^{-1}$	$\alpha = 0.25$	1
$Na_xE_1 \rightleftharpoons Na_xE_1ATP$	a	$K_a = 0.5\ \mu M$	$3.5 \times 10^6\ M^{-1}s^{-1}$	0	2
$Na_3E_1ATP \rightleftharpoons (Na_3)E_1$-P	p	$K_p = 2.5 \times 10^3\ M^{-1}$	$600\ s^{-1}$	0	3
$(Na_3)E_1$-P $\rightleftharpoons$ P-$E_2(Na_3)$	l	$K_l = 0.11$	$25\ s^{-1}$	$\beta = 0.1$	4
P-$E_2(Na_3) \rightleftharpoons$ P-$E_2(Na_2)$	g_3	$K_{g3} = 10\ M^{-1}$	$1.4 \times 10^3\ s^{-1}$	$\delta_0 = 0.65$	4
P-$E_2(Na_2) \rightleftharpoons$ P-$E_2(Na)$	g_2	$K_{g2} = 0.65\ M^{-1}$	$5.0 \times 10^3\ s^{-1}$	$\delta_1 = 0.1$	4
P-$E_2(Na) \rightleftharpoons$ P-E_2	g_1	$K_{g1} = 11.1\ M^{-1}$	$7.0 \times 10^2\ s^{-1}$	$\delta_2 = 0.1$	4
P-$E_2 \rightleftharpoons E_1$	r	$K_r = 4.3 \times 10^4\ M^{-1}$	$0.023\ s^{-1}$	$\gamma = 1.8$	5
P-$E_2(Na_2) \rightleftharpoons E_2(Na_2)$	d	[#]	$1.4\ s^{-1}$	0	2
$E_2(Na_2) \rightleftharpoons Na_2E_1$	e	$K_e = 5$	$50\ s^{-1}$	0	2

The rate constants (n_{3f}, a_f, p_f, . . .) and the equilibrium constant (K_{n3}, K_a, K_p, . . .) were determined at 22°C. These parameters were used in the numerical simulations presented in this paper, according to the pump cycle of Fig. 1.

*Not determined, cytoplasmic Na^+ binding is fast compared to the reaction steps and therefore is treated as an equilibrium reaction controlled by K_1.

[#]Not determined, because $[P_i] = 0$.

[§]References are taken from 1: Schulz and Apell (1995). 2: Heyse et al. (1994). 3: This work. 4: Wuddel and Apell (1995). 5: Apell et al. (1996).

nylbenzofuran, was prepared as described (Sheehan et al., 1971). For experiments in which the by-product was added to membrane preparations, it was dissolved in ethanol to form a stock solution at a concentration of 8 mM.

Na,K-ATPase preparation and specific activity

Na,K-ATPase was prepared from the outer medulla of rabbit kidneys by procedure C of Jørgensen (1974). This method yielded purified enzyme in the form of membrane fragments, which consisted of flat sheets with a diameter of 0.2–1 μm, and contained ~0.8 mg phospholipid and 0.2 mg cholesterol/mg protein (Bühler et al., 1991). The suspension of membrane fragments containing Na,K-ATPase (~3 mg total protein/ml) in buffer (25 mM imidazole sulfate, pH 7.5, 1 mM EDTA, 10 mg/ml sucrose) was frozen in 100-μl aliquots; in this form the preparation could be stored for several months at −70°C without significant loss of activity. Storage of thawed preparations at +4°C for up to 4 weeks did not affect the activity. The protein concentration was determined by the Lowry method (Lowry et al., 1951), using bovine serum albumin as a standard. The Na,K-ATPase specific activity was determined by the pyruvate kinase/lactate dehydrogenase linked assay (Schwartz et al., 1971). For all preparations, the specific activity was in the range of 1900–2300 μmol P_i formed/h/mg protein at 37°C and pH 7.5. This corresponds to a k_{cat} of 72–86 s^{-1}, based on two active sites, and a molecular mass of 270 kDa for the ATPase dimer (Jørgensen, 1974). At 22°C the specific activity was 630 μmol P_i formed/h/mg protein, which corresponds to a k_{cat} of 24 s^{-1}. Between pH 6 and 8.25 the specific activity-pH profile was approximately bell shaped (see data plotted in Fig. 5 *b*, and Apell and Marcus, 1986). For measurements at pH values other than 7.5, control experiments were performed to ensure that the linked-assay enzymes were not rate limiting.

Membrane experiments

The apparatus was described previously (Borlinghaus et al., 1987; Wuddel and Apell, 1995); Fig. 2 *a* summarizes essentials of the two-compartment cell. The cell made of Teflon 228 was mounted in a thermostatted aluminum block in a Faraday cage. Planar lipid bilayers were formed from 1% diphytanoylphosphatidylcholine in *n*-decane across a hole of 1-mm diameter in the wall between the front (*trans*) and back (*cis*) compartments and were illuminated and observed through quartz windows in the *trans* compartment. The area of the optically black bilayers was typically 0.55 mm^2. The standard buffer composition between pH 6 and pH 7.5 was 30 mM imidazole, 10 mM $MgCl_2$, and 1 mM EDTA, with specified concentrations of NaCl, and the temperature was 22°C. The buffer agent was 2-(*N*-morpholino)ethanesulfonic acid (30 mM) at pH < 6 and Tris (30 mM) at pH > 7.5. Except when stated, transient current experiments were performed in the absence of K^+ (apart from any added as the counterion to DMB-caged ATP), which restricted the ion pump to its Na-only mode. The effect of K^+ counterion at the concentrations added with the DMB-caged ATP would have a negligible effect on transient amplitudes and kinetics (Borlinghaus et al., 1987). The potential across the bilayer was detected with Ag/AgCl electrodes; we shielded these against stray-light artifacts by embedding them in agar gel stained black with ink. Light from a flash lamp (model 5M-3; EG&G Electro Optics, Salem, MA) was transmitted through a 1-mm-pathlength bandpass filter (270–380 nm; Schott UG 11) and focused on the membrane. The *cis* compartment, which had a volume of ~300 μl, was equipped with a small magnetic stirrer. After a bilayer was formed, caged ATP, 0.4 units (manufacturer's specification) of apyrase, and 40–50 μg/ml membrane fragments were added to the *cis* side, followed by 1 min of smooth stirring. Apyrase was added to remove ATP and ADP efficiently (Borlinghaus et al., 1987) unless otherwise stated. Membrane fragments adsorbed to the lipid bilayer with a time constant of several minutes (Borlinghaus et al., 1987). Neither DMB-caged ATP nor NPE-caged ATP affected the membrane resistance or capacitance of the preparation.

Transient currents were triggered by a light flash that photolyzed caged ATP and produced an ATP concentration jump in the close vicinity of the membrane fragments adsorbed in the bilayer. Experiments were performed after an equilibration period of at least 10 min after the addition of the fragments. Typical lifetimes of the coupled membrane systems were 120–240 min. During this time the maximum amplitude of the transient currents slowly decreased, but their kinetics were unaltered. The currents detected after an ATP-concentration jump are directly proportional to the number of participating pump molecules. This number varied significantly between various membranes under otherwise constant conditions, because of the different extents of membrane fragment adsorption (see text below associated with Fig. 4).

Charge movements within the ion pumps in the membrane fragments could be detected as changes in the transmembrane electric voltage by the principle of capacitive coupling, as discussed previously (Borlinghaus et al., 1987; Wuddel and Apell, 1995). Thus charge movements were recorded either as voltage changes by a voltage amplifier on the basis of an operational amplifier with an input impedance of $10^{12}\ \Omega$ (Burr Brown 3528, Tucson, AZ), or as current changes by a current amplifier with a gain of 10^9 V/A and a signal rise time set at 1–3 ms (model 427; Keithley, Cleveland, OH). Signals recorded in the latter way had a lower signal-to-noise ratio at the same cutoff frequency compared to the voltage traces, but could be analyzed directly. Current and voltage signals were fully comparable (Wuddel and Apell, 1995). The output signal was recorded by a digital oscilloscope (model 4094A; Nicolet, Madison, WI) after the trigger

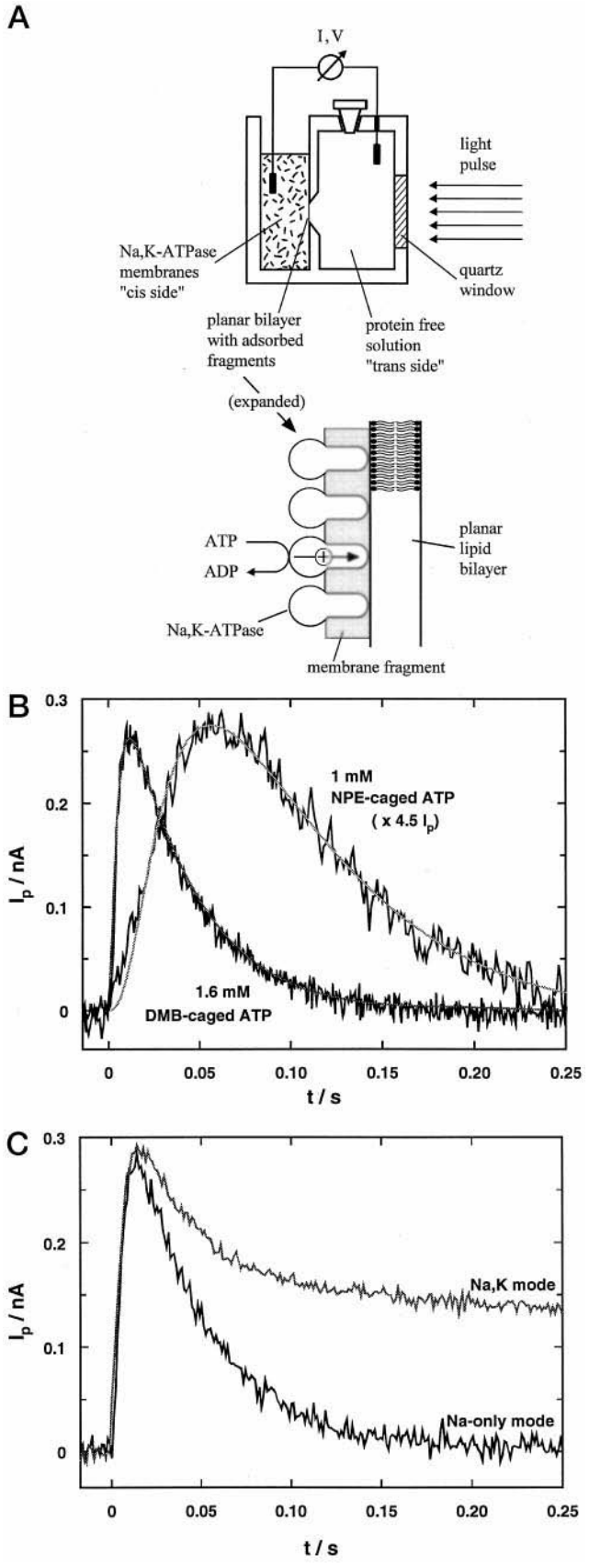

FIGURE 2 Comparison of ATP-induced current transients produced by Na,K-ATPase. (*a*) The two-compartment cell for current measurements expanded at planar bilayer to show the capacitively coupled membrane fragments (Borlinghaus and Apell, 1988; Wuddel and Apell, 1995). (*b*) The currents were triggered by ATP concentration jumps generated by flash photolysis of two caged ATP compounds, DMB-caged ATP and NPE-caged ATP. Experiments were performed in standard buffer containing 150 mM NaCl and the indicated concentration of the caged compound (pH 7.5, 22°C). ATP at 100 μM and 80 μM was released from DMB-caged ATP and NPE-caged ATP, respectively. The lines plotted through the data are simulations of the experiments according the reaction scheme of Fig. 1, the experimental conditions, and the parameters listed in Table 1. (*c*) Currents following 100 μM ATP concentration jumps generated by flash photolysis of DMB-caged ATP in standard buffer at 22°C containing 100 mM NaCl plus 50 mM KCl in the Na^+,K^+ mode and 150 mM NaCl in the Na^+-only mode. In both *b* and *c* the light flash is at time 0 on the abscissa.

of a 40-μs near-UV flash. For more details refer to Wuddel and Apell (1995).

Data analysis

Unless otherwise stated, errors are recorded as SEM and are derived from at least four trials at the recorded concentration or pH. Data were analyzed on a personal computer. The recorded voltage signals were transformed into current, $I(t)$, and according to a published formalism into pump-current signals, $I_p(t)$ (Borlinghaus and Apell, 1988). The transients obtained were compared to the results of a kinetic simulation of the model shown in Fig. 1, based on the rate constants (Table 1) and programs of Wuddel and Apell (1995), but with modifications that became necessary because of revised values for λ (see Appendix) and the experimental findings presented in this paper. Under standard conditions (pH 7.5, 22°C), only the rate constants of enzyme phosphorylation by ATP, p_f, and enzyme dephosphorylation by ADP, p_b, had to be modified.

RESULTS

Comparison of transient currents induced by photolysis of NPE- and DMB-caged ATP

The membrane fragments containing Na,K-ATPase adsorbed to the lipid bilayer are shown schematically in Fig. 2 *a*. Fig. 2 *b* shows the results of experiments in the standard buffer at pH 7.5, which contained 150 mM NaCl. In both experiments, 40 μg/ml Na,K-ATPase in the form of membrane fragments and the indicated amount of caged ATP (1 mM NPE-caged ATP or 1.6 mM DMB-caged ATP) were added to the *cis* side. Transient voltage changes were recorded after a 40-μs light flash at time $t = 0$. Numerical differentiation of the voltage signal according to the procedure of Borlinghaus and Apell (1988) gave the current transients shown. The currents rose to a maximum within 10 ms (DMB-caged ATP) and 60 ms (NPE-caged ATP) and thereafter declined, reversing their sign at $t > 150$ ms or $>$ 250 ms, respectively. In the representation of Fig. 2 *b* the pump-current trace of the NPE-caged ATP has been scaled up 4.5-fold to make the different time courses more readily visible.

The yield of photoreleased ATP, ϑ, from caged ATP in the experimental setup was determined by photolyzing 5-μl droplets placed at the position of the hole spanned by the membrane. The droplet contained standard buffer and 1 mM NPE-caged ATP or 1.6 mM DMB-caged ATP. Different

settings of the flash-lamp voltage gave ϑ values up to 0.07 for DMB-caged ATP. The concentration of released ATP was determined by a luciferase bioluminescence assay. The ratio of ATP released from NPE-caged ATP to that from DMB-caged ATP was 1.2 ± 0.2 over a 0.1–1.6 mM concentration range of caged compound. The concentrations of ATP released in the Na,K-ATPase studies that follow were calculated from these data.

The influence of K^+ on the current measured using NPE-caged ATP has been described (Fendler et al., 1985, 1987; Borlinghaus et al., 1987). Fig. 2 *c* shows a comparison of currents observed after photolysis of DMB-caged ATP with and without 50 mM KCl. In the presence of KCl, a steady-state current occurs because of cycling of the Na,K-ATPase. Additional ATP released in the presence of K^+ by a second flash did not increase the steady-state current (data not shown), indicating that ATP was not limiting. The current declined to zero by 1.5 s. The additional current contributions arose from turnovers in the Na-K mode of the pump until the small aqueous volume between lipid bilayer and membrane fragments was depleted of K^+ ions. This extended pump activity is in agreement with previously published findings for NPE-caged ATP (Fendler et al., 1985, 1987; Borlinghaus et al., 1987). The early part of the current response to photolysis of DMB-caged ATP was little affected by K^+, a result comparable to that of experiments in which NPE-caged ATP was used.

Several controls were performed to ensure that the transient currents were exclusively produced by the ion-translocating action of the Na,K-ATPase. First, experiments using DMB-caged ATP were performed in the absence of Mg^{2+} (which is required for phosphorylation of the enzyme). Under these conditions, no flash-induced signal was observed, apart from a negative current spike artifact of less than 3 ms duration (see below); subsequent addition of 10 mM Mg^{2+} to the *cis* buffer restored the photolytically induced response with normal kinetics (data not shown), although the signal amplitudes were smaller than in experiments with Mg^{2+} present from the beginning. This difference probably originates from the less effective adsorption of membrane fragments to the lipid bilayer in the absence of divalent ions; these ions may produce an electrostatic attraction between fragment and bilayer (Wuddel, 1994).

To test whether binding of DMB-caged ATP to the nucleotide binding site inhibits Na,K-ATPase, the specific enzymatic activity was measured in the presence of increasing amounts of the caged compound. There was no significant decrease in the enzyme activity up to 0.75 mM DMB-caged ATP, the highest concentration used (0.2 mM ATP in the assay).

On photolysis of DMB-caged ATP, the by-product, 5,7-dimethoxy-2-phenylbenzofuran, was expected to become rapidly incorporated into the membrane because of its hydrophobicity and to possibly interfere with protein function. The specific activity of the Na,K-ATPase was unaffected by the presence of 200 μM 5,7-dimethoxy-2-phenylbenzofuran, a concentration higher than any liberated in the DMB-caged ATP experiments. Control experiments were performed with bilayers in the presence of benzofuran but in the absence of DMB-caged ATP. Under these conditions the spike artifact mentioned above was observed, and its time course and size corresponded to those in the experiments with membrane fragments containing Na,K-ATPase and DMB-caged ATP. Thus the spike artifact was attributable to the by-product; its amplitude was variable, being barely detectable in most experiments. Consequently, measurements with membranes that showed a large light-induced artifact were discarded. The mechanism giving rise to the artifact has not been further studied.

To investigate further the effect of the different rates of ATP release, the dependence of the transient currents on the concentration of the two caged compounds was determined (Figs. 3 and 4). Fig. 3 shows transients from trials with 0.2–2.4 mM DMB-caged ATP. To characterize the transients, two parameters, the maximum current, I_{max}, and the time between the light flash and the maximum current, t_{max}, were determined (see *inset* in Fig. 3). They were obtained from a fitting routine, in which the transient current was reduced to two exponentials:

$$I_p(t) = I_o(\exp(-k_2 t) - \exp(-k_1 t)) \quad (1)$$

I_o, k_1, and k_2 are fitted parameters. I_o is proportional to the number of activated ion pumps (see Eq. 4). As expected from the multistep reaction, Eq. 1 is an oversimplification, because the rising phase was not a single exponential process (as illustrated in the *inset* of Fig. 3), either experimentally or when simulated as in Fig. 2 *b* (according to the method of Wuddel and Apell, 1995). Nevertheless, Eq. 1 provides a convenient parameterization both of experimen-

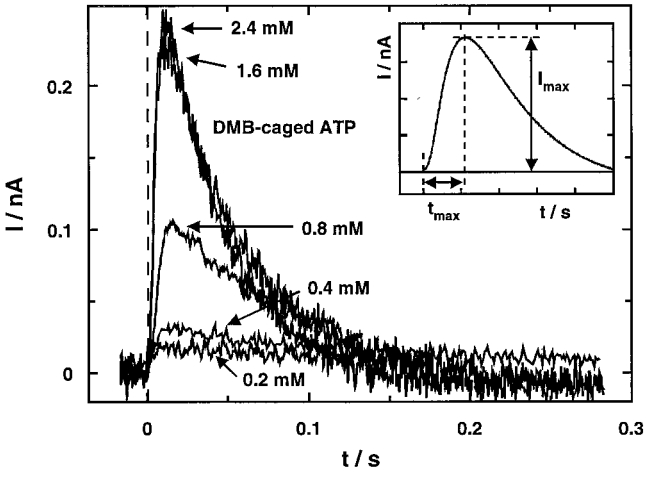

FIGURE 3 Transient currents in response to a light flash in the presence of different concentrations of DMB-caged ATP. The aqueous solution contained standard buffer with 150 mM NaCl, membrane fragments (40 μg/ml Na,K-ATPase), and the indicated concentration of DMB-caged ATP at pH 7.2 and 22°C. The time of the light flash is zero on the abscissa. I_{max} and t_{max} were determined from the transients as characteristic parameters (see *inset*).

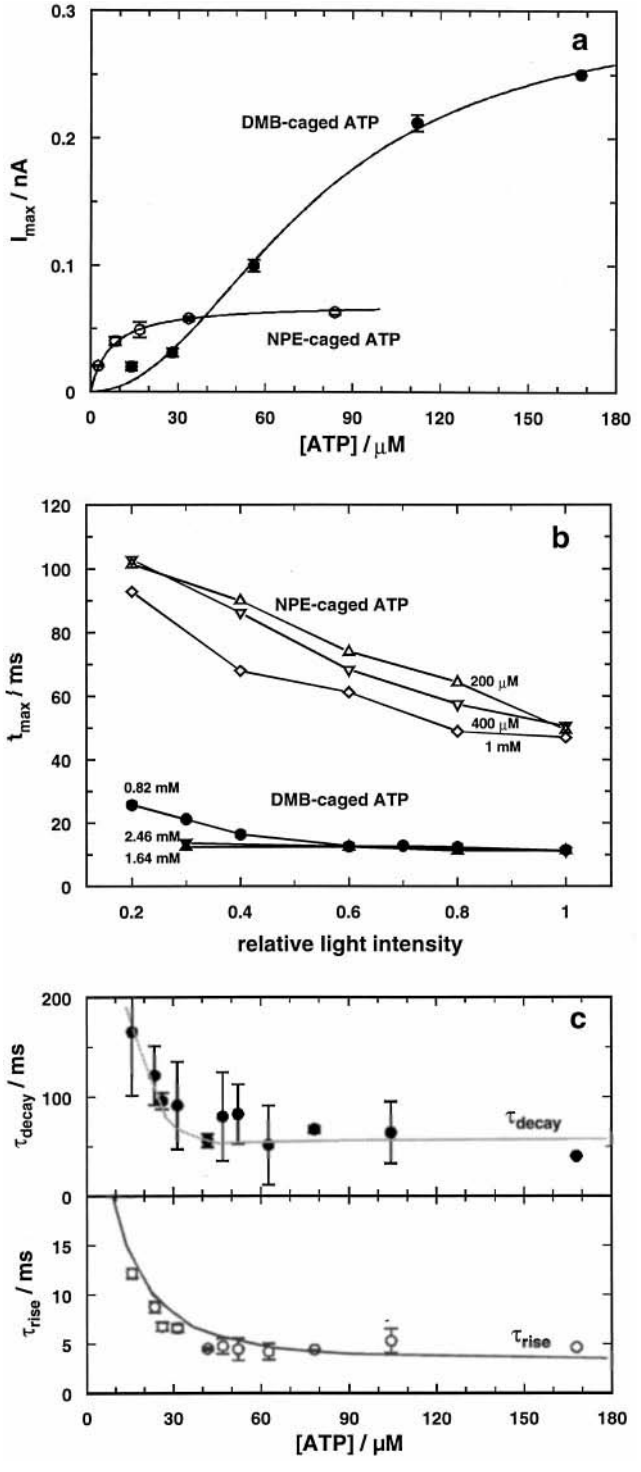

FIGURE 4 (*a*) Dependence of I_{max} on concentration of released ATP from DMB-caged ATP (●) and NPE-caged ATP (○) at constant light-flash intensity ($\vartheta = 0.07$ for DMB-caged ATP and $\vartheta = 0.082$ for NPE-caged ATP). The DMB-caged ATP data are averaged from transients as shown in Fig. 3. The error bars are SEM derived from several transients at a constant caged ATP concentration in a single membrane experiment. The lines are drawn to guide the eye. (*b*) Dependence of t_{max} on concentration of caged ATP and the relative intensity of the light flash. DMB-caged ATP (●, ▲, ▼) and NPE-caged ATP (◇, △, ▽) data are compared under otherwise identical conditions (as described in legend of Fig. 3). The light-flash intensity was varied to generate yields of released ATP between 1.6% and 8% of the concentration of caged compounds. In each case a relative light intensity of 1 corresponded to the same light intensity. (*c*) Analysis of the current transients, $I(t)$, by fits with Eq. 1. The fit parameter τ_{rise} and τ_{decay} are plotted against the concentration of ATP released from various DMB-caged ATP concentrations and light intensities as in *b*. The lines are derived from simulated current transients at different ATP concentrations according to the model described in the Appendix, which were then fitted by Eq. 1. Large errors in τ_{decay} are related to the low current amplitudes at less than 60 μM ATP seen in *a*.

tal data and of simulated transients derived from the model scheme (Fig. 1). t_{max} and I_{max} may be expressed in terms of k_1 and k_2 as follows:

$$t_{max} = \ln(k_1/k_2)/(k_1 - k_2) \quad (2)$$

$$I_{max} = I_o \cdot ((k_1/k_2)^{-k_2/(k_1-k_2)} - (k_1/k_2)^{-k_1/(k_1-k_2)}) \quad (3)$$

where

$$I_o = e_o N \cdot k_1 k_2/(k_1 - k_2). \quad (4)$$

The dependence of I_{max} on the concentration of released ATP is shown in Fig. 4 *a*. These experiments were performed for a sequence of caged ATP concentrations by successive additions of caged compound to the same membrane. As noted in Materials and Methods, this procedure was necessary for internal consistency of the data set, because variation of I_{max} between different membranes can be large because of a variable amount of adsorbed membrane fragments (i.e., the number of activated pumps; see Eqs. 3 and 4). Therefore I_{max} at any particular concentration of released ATP is not reproducible unless it is recorded from the same bilayer experiment. Saturation of I_{max} occurred on NPE-caged ATP photolysis with half-saturating amplitude on release of 5 μM ATP (Fig. 4 *a*). With DMB-caged ATP concentrations, there was only a tendency toward saturation of I_{max} with half-saturating amplitude on release of ~70 μM ATP. In contrast, t_{max} was constant within experimental error over the range of applied concentrations of DMB-caged ATP (200 μM to 2.46 mM), with an average value of 11.1 ± 0.1 ms, derived from fits of Eq. 1 to the data of Fig. 3 and calculations using Eq. 2. In parallel experiments using NPE-caged ATP, t_{max} was weakly dependent on the concentration of caged compound decreasing from 75 ± 6 ms to 45 ± 4 ms between 33 μM and 1 mM NPE-caged ATP, respectively (data not shown; see also data in Fig. 4 *b*).

Changes in t_{max} might be expected if the association of photoreleased ATP with Na,K-ATPase was inhibited by binding of DMB-caged ATP to the nucleotide site, a process known to occur with NPE-caged ATP (Forbush, 1984a). Borlinghaus and Apell (1988) have shown that the yield of photoreleased ATP is proportional to the intensity of the light flash, so the light flash intensity was varied fivefold over a range of caged ATP concentrations, and t_{max} was plotted against the relative light intensity (Fig. 4 *b*). Binding of NPE-caged ATP to the Na,K-ATPase influenced the kinetics because t_{max} observed at 1 mM NPE-caged ATP and relative light intensity 0.2 was twice that at 200 μM and light intensity 1. Similar experiments performed with DMB-

caged ATP demonstrated less influence of its concentration on t_{max}. The average t_{max} value (with the exception of experiments at 0.82 mM and relative intensity < 0.4) was 12.0 ± 0.28 ms. Thus putative binding of DMB-caged ATP to the ATP site did not significantly influence t_{max} values. Values of t_{max} for the transient currents upon photorelease of ATP from DMB-caged ATP were at least 3.5-fold less than t_{max} values observed on photolysis of NPE-caged ATP at each light intensity. Furthermore, with NPE-caged ATP, the average ratios of the t_{max} values at each light intensity were 1.22:1.15:1 for 0.2, 0.4, and 1 mM NPE-caged ATP, respectively, confirming that the transients were significantly affected by the kinetics and/or amount of ATP release and not just by binding of NPE-caged ATP to the nucleotide site of the ATPase.

The current transients were also recorded in terms of the time constants τ_{rise} ($= 1/k_1$) and τ_{decay} ($= 1/k_2$) of the rising and falling phase (Fig. 4 *c*). Both parameters show an increase for concentrations of released ATP below 40 μM.

Dependence of transient currents on pH

Transient currents were compared after flash photolysis of DMB-caged ATP in the presence of 150 mM NaCl at various pH values (Fig. 5 *a*). Between pH 5.3 and pH 8.0, no marked changes were observed in t_{max} when ATP was released from DMB-caged ATP; however, a threefold increase in t_{max} occurred between pH 8 and pH 9 (Fig. 5 *b*). Similar experiments have been performed with NPE-caged ATP (Borlinghaus et al., 1987), and those results are shown for comparison in Fig. 5 *b*. Values of t_{max} coincided for both compounds at pH $\leq$ 6, where the photolysis rate of NPE-caged ATP is greater than 2000 s^{-1} (Walker et al., 1988), whereas as expected, t_{max} values diverged above pH 6 for the two caged compounds. Because the pH dependence of the Na,K-ATPase activity (recorded in Materials and Methods) is relevant to the discussion of the transient currents, reciprocal enzyme activities are also plotted in Fig. 5 *b*. I_{max} increased by a factor of 4 between pH 6 and pH 8 (Fig. 5 *a*), an effect that is most likely due to the more than twofold increase in enzyme activity and variation with pH in the adsorption of membrane fragments to the lipid bilayer.

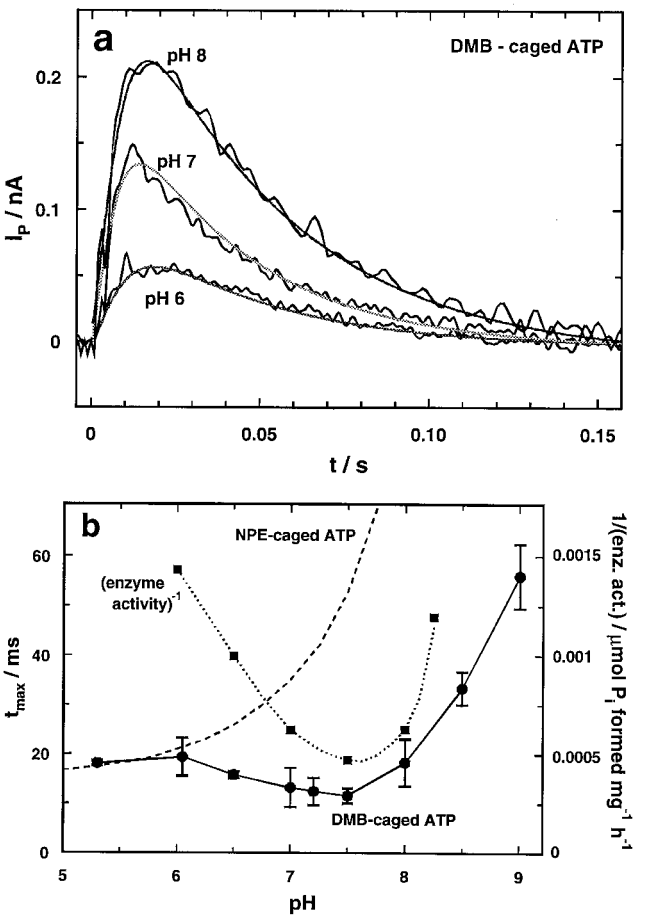

FIGURE 5 Dependence of transient currents on pH after flash photolysis of 0.8 mM DMB-caged ATP. (*a*) Transient currents at pH 6, 7, and 8 on release of 55 μM ATP. Apart from pH, other conditions were as described in the legend of Fig. 3. The smooth lines drawn through the experimental traces are simulations derived as described in the Appendix. (*b*) t_{max} is plotted as a function of pH (●). The line has been drawn to guide the eye. Results obtained from similar experiments with NPE-caged ATP, which are reproduced from Borlinghaus and Apell (1988), are shown for comparison (*dashed line*). The pH dependence of the enzyme activity has been determined (see Materials and Methods), and the reciprocal values, which are proportional to the cycle time of the Na,K-ATPase, are plotted as solid squares (and as a *dotted line* to guide the eye).

Dependence of transient currents on sodium concentration

As considered in the Introduction, the characteristics of the transient currents are likely to be influenced by the initial concentration of Na_3E_1. Therefore transient currents after DMB-caged ATP photolysis were analyzed as a function of Na^+ concentration. t_{max} decreased with increasing Na^+ concentration from 73 ms (1 mM Na^+) to 8.6 ms (50 mM Na^+) and increased at higher Na^+ (35 ms at 400 mM). t_{max} is plotted as $1/t_{max}$ in Fig. 6 *a* to allow direct comparison with data obtained using NPE-caged ATP under otherwise comparable conditions (Borlinghaus and Apell, 1988). In the earlier work, the transients were not influenced by ionic strength (up to 250 mM), so no compensation for changing ionic strength was made here in the DMB-caged ATP experiments. In Fig. 6, *b* and *c*, the effects of the Na^+ concentration on τ_{rise} and τ_{decay} are shown. Between 2 mM and 150 mM NaCl, τ_{rise} varied by more than factor of 10, whereas τ_{decay} (60 ± 8 ms) did not change significantly.

Dependence of transient currents on ADP concentration

The phosphorylation $Na_3E_1ATP \rightleftharpoons (Na_3)E_1\text{-}P + ADP$ may be affected by the presence of ADP, and the contribution of the back-reaction to the reaction flux allows an estimate of the corresponding rate constant p_b. Therefore experiments

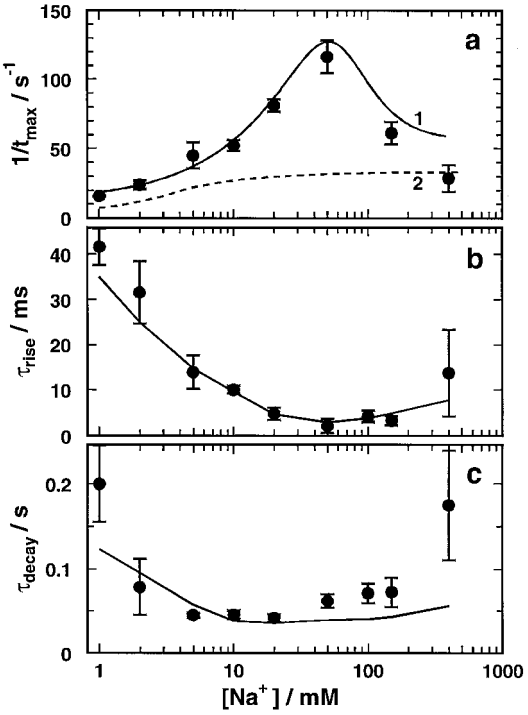

FIGURE 6 Dependence of transient currents on Na^+ concentration. (*a*) $1/t_{max}$ is plotted against Na^+ concentration (●) after release of 55 μM ATP from 0.8 mM DMB-caged ATP (*trace 1*). All other conditions are as described in the legend of Fig. 3. For comparison the results obtained from similar experiments with NPE-caged ATP (195 μM ATP released; Borlinghaus and Apell, 1988) are shown as a dashed line (*trace 2*). (*b*, *c*) Transients were fitted according to Eq. 1, and the derived rate constants, k_1 and k_2, were used to calculate the characteristic time constant of the rising phase, $\tau_{rise} = 1/k_1$, and of the falling phase, $\tau_{decay} = 1/k_2$. The solid lines in all three panels derive from simulated transients at different sodium concentrations according to the model described in the Appendix, which were then fitted by Eq. 1 to obtain the plotted $1/t_{max}$, τ_{rise}, and τ_{decay}.

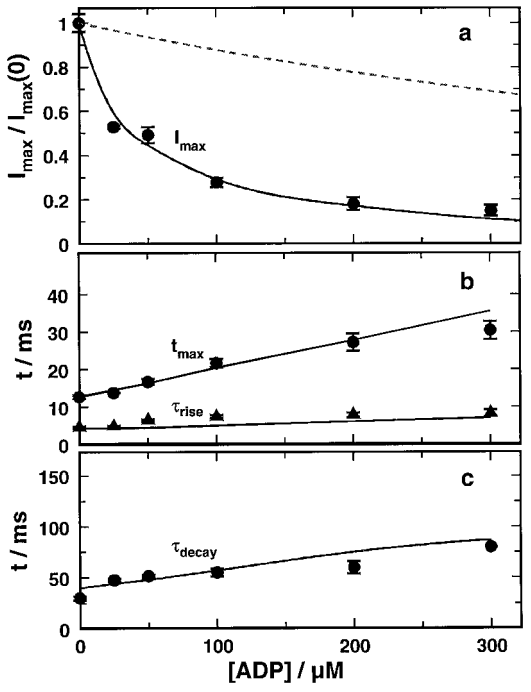

FIGURE 7 Dependence of transient currents on concentration of added ADP. Transients triggered by release of 55 μM ATP from 0.8 mM DMB-caged ATP were recorded in the presence of the indicated concentrations of ADP and analyzed by fits of the time course with the function of Eq. 1. Other conditions were as described in the legend to Fig. 3. It was estimated that less than 10 μM ADP was present as a contaminant in the DMB-caged ATP, and thus it was ignored. The characteristic parameters of current transients are (*a*) the maximum current amplitude normalized to that at zero [ADP], I_{max}/I_{max} (0); (*b*) t_{max} and τ_{rise} ($= 1/k_1$); (*c*) τ_{decay} ($= 1/k_2$). The solid lines in all three panels were obtained as in Fig. 6, except that ADP rather than Na^+ concentrations were varied to obtain the plotted $I_{max}/I_{max}(0)$, t_{max}, τ_{rise}, and τ_{decay}. The dashed line in *a* represents a calculated inhibition for the hypothetical case that the phosphorylation rate constant, p_f, is slow and the conformational change rate constant, l_f, is fast (see Discussion).

were performed with release of 55 μM ATP from DMB-caged ATP in the presence of various concentrations of ADP, without apyrase. The dependence of the transient currents on ADP was analyzed and represented in the parameters I_{max}, t_{max}, τ_{rise}, and τ_{decay} (Fig. 7). In a series of experiments with the same membrane preparations (to maximize reproducibility), I_{max} measured in the presence of 300 μM ADP was 15% of its value with no added ADP. Over the range 0–300 μM ADP t_{max}, τ_{rise} and τ_{decay} increased 2.5-, 1.8-, and 2.6-fold, respectively.

DISCUSSION

A variety of Na,K-ATPase preparations and experimental techniques have been used to analyze the kinetics of electrogenic Na^+ transport in Na,K-ATPase (Forbush, 1984b; Fendler et al., 1985, 1987, 1993; Nakao and Gadsby, 1986, 1989; Borlinghaus et al., 1987; Borlinghaus and Apell, 1988; Rakowski et al., 1991; Stürmer et al., 1991; Vasilets et al., 1991; Gadsby et al., 1993; Heyse et al., 1994; Hilgemann, 1994; Sagar and Rakowski, 1994; Wuddel and Apell, 1995). To obtain quantitative information on rate constants of the Na^+-translocating reaction cycle, Wuddel and Apell (1995) fitted data from a wide range of experiments to the Na-only mode of Na,K-ATPase (Fig. 1 and Table 1). In such experiments the system was perturbed from its steady state by a sudden change in an external parameter, such as temperature, voltage, or a substrate concentration, and the time evolution of the system toward a new steady state was followed (Läuger, 1991). Most of the experiments presented in this paper (when [Na^+] > 20 mM) relate to the following steps:

$$Na_3E_1 \rightleftharpoons Na_3E_1ATP \rightleftharpoons (Na_3)E_1\text{-}P \rightleftharpoons P\text{-}E_2(Na_3) \rightleftharpoons P\text{-}E_2$$

The application of NPE-caged ATP has been a powerful tool for determining kinetic properties of Na^+ transport in Na,K-ATPase. However, the time course of ATP release must explicitly be taken into account when transient currents are analyzed (Borlinghaus and Apell, 1988; Wuddel and Apell, 1995). Possible distortion of the transients can be minimized by use of DMB-caged ATP, which photolyzes at

least three orders of magnitude more rapidly than NPE-caged ATP at physiological pH. The various control experiments established that DMB-caged ATP and its photolysis by-product were innocuous with respect to the electrical properties of the Na,K-ATPase capacitively coupled to a bilayer. Significantly, when ATP was released from DMB-caged ATP in the absence of Mg^{2+}, no transient currents were observed. Upon addition of Mg^{2+}, the pump-induced transient was restored. Likewise, the effect of K^+ on the steady-state current after photolysis of DMB-caged ATP, together with its lack of effect on the kinetics and amplitude of the transient current, is compatible with the expected properties of K^+ in the Na,K-ATPase mechanism. These observations on the influence of Mg^{2+} and K^+ agree with data from NPE-caged ATP (Fendler et al., 1985, 1987; Borlinghaus et al., 1987).

Shape of the transient current

Fig. 2 *b* demonstrates that the shape of the transient currents in experiments is different for the two caged ATP analogs. Overall the transient was faster and the maximum current amplitude, I_{max}, much greater with DMB-caged ATP. The latter follows from the former, because the integral of the current, other things being equal, will be the same. However, we found variations in I_{max} and the current integral, because both are proportional to the number of contributing ion pumps (i.e., the density of adsorbed membrane fragments), and this is known to vary from experiment to experiment and over time within a single membrane.

The faster transient currents with DMB-caged ATP are most likely to arise from its more rapid photolysis. However, we also have to consider the extent to which binding of the caged ATP compounds to the ATP site on the pump influences the kinetics. For NPE-caged ATP, competition between ATP and the caged compound has been shown, and dissociation constants for NPE-caged ATP in the range 40–500 μM have been determined (Forbush, 1984a; Borlinghaus and Apell, 1988). Nevertheless, t_{max} is only twice as large when fivefold greater NPE-caged ATP is present for the same amount of released ATP (cf. data of 200 μM and 1 mM caged ATP in Fig. 4 *b*). Part of this relative insensitivity probably arises because of the nonlinear relation between t_{max} and $1/k_1$ (or $1/k_2$) (Eq. 2). Thus suppose that $k_1 \gg k_2$, and k_1 was proportional to [caged ATP]; then the t_{max} would not have a linear dependence on 1/[caged ATP], because $t_{max} \propto \ln(k_1)/k_1$. Furthermore, phosphorylation may be partially rate limiting in steps leading up to the formation of $(Na_3)E_1$-P. In the case of DMB-caged ATP, even less effect on t_{max} was found when the same amount of ATP was released from varying concentrations of caged ATP with correspondingly adjusted flash intensity. This result is still compatible with weak binding of DMB-caged ATP to the ATP site. We simulated transient currents to estimate the effect of the DMB-caged ATP dissociation constant on t_{max}. The simulations indicated that t_{max} was >13 ms for values ≤ 5 mM, suggesting that this is a lower limit for the dissociation constant. It is noteworthy that DMB-caged ATP and NPE-caged ATP have comparable affinities for the myosin ATP binding site (Thirlwell et al., 1995). We conclude that the principal cause for the different kinetics of the transient currents is the slower ATP release from NPE-caged ATP.

When an activation energy of 100 kJ/mol (Linder and Apell, manuscript in preparation) is applied for the rate-limiting process, for comparison the rate constants at 22°C can be estimated from published data. They vary between 200 s^{-1} (Fendler et al., 1987), 70 s^{-1} (Hilgemann, 1994), 40 s^{-1} (Gadsby et al., 1991), and 25 s^{-1} (Heyse et al., 1994; Wuddel and Apell, 1995; this work). Friedrich and Nagel (1997) recently published transient current experiments performed with giant patches from myocytes. They observed transient kinetics similar to those presented here ($\tau_{rise} = 6$ ms, $\tau_{decay} = 25$ ms at 20°C, 55 μM ATP released); however, they assigned the slow falling phase of the current to binding/dissociation of ATP/caged ATP to/from the enzyme. The origin of the discrepancies in the rate-limiting step still has to be resolved. When the effect of the slow photolysis of NPE-caged ATP is excluded (as in the presented data), two other factors may contribute to reduce the limiting rate: caged ATP (NPE- or DMB-caged ATP) has a kind of "allosteric" inhibition effect on our preparation, which slows down the rate-limiting conformational change. If so, one would expect to detect a concentration dependence of the inhibition, which was not found in the concentration range of the caged compound between 0.2 mM and 2.4 mM by electric measurements (Fig. 4 *b*), or at concentrations lower than 0.75 mM in the overall enzymatic activity. From the absence of any observed concentration dependence it may be excluded that this process produced a change of the limiting rate in the order of a factor of 10. The second factor may be the difference between native membranes (as used by Hilgemann, 1994, or Gadsby et al., 1991) and our purified microsomal preparations in which the lipid composition is significantly altered. This could easily account for the observation of a factor on the order of 2 between Hilgemann's, Gadsby's, or Friedrich's results and ours. However, this cannot explain the difference of a factor of 10.

Simulations of the Na-only mode of Na,K-ATPase

From Fig. 2 *b* it can be seen that both the rising and falling phases of the transient current are affected by the ATP-release kinetics. To quantify the differences in the current traces, fits were performed of the time course of the signals according to the function given in Eqs. 1 and 2 to determine the parameters I_{max}, t_{max}, τ_{rise} ($= 1/k_1$), and τ_{decay} ($= 1/k_2$). These fits were acceptable in most cases, although in experiments with high time resolution, it could be seen that the rising phase of the current deviated considerably from the fitted curve for experiments with DMB-caged ATP. This is

not surprising, because the underlying transport process from Na_3E_1 to P-E_2 in Na,K-ATPase is at least a four-step reaction, so reduction of the kinetic scheme to two rate constants is an oversimplification; k_1 and k_2 are necessarily complex functions of all rate constants.

To demonstrate the influence of the rate constants of the reaction scheme on the rising and falling phases of the transient currents, we performed numerical simulations with the reaction scheme of Fig. 1 and the parameters of Table 1 in the way presented in the Appendix for DMB-caged ATP. The reaction steps of the pump cycle that are not part of the linear sequence from Na_3E_1 to P-E_2 did not contribute significantly to the simulations of the whole cycle at 150 mM Na^+. Just as for the measured transient currents, the simulated time courses of the scheme in Fig. 1 were fitted with Eq. 1 to determine the apparent time constants, τ_{rise} and τ_{decay}. These parameters were then plotted as functions of three rate constants of the reaction scheme (Fig. 8). The rate constants a_f and p_f may be varied by a factor of 2 to either side of their values in Table 1 (*arrows* in Fig. 8) without modifying τ_{rise} and τ_{decay} significantly. Similar twofold variations in the rate constant l_f have no effect on τ_{rise} but significantly affect τ_{decay}. Repetition of these simulations (not shown), with the slower ATP release kinetics of NPE-caged ATP (see Appendix), led to a comparable result, with the only difference that τ_{rise} and τ_{decay} increased, as observed experimentally (Fig. 2 *b*). The apparent biphasic dependence of τ_{decay} in Fig. 8 *a* and the decreasing τ_{decay} for small p_f in Fig. 8 *b* are the consequence of inadequacy of the function in Eq. 1 discussed above.

In summary, the slow release of ATP from NPE-caged ATP reduced the overall rate of the transient current compared to DMB-caged ATP. The kinetics of the rising phase of the transient current cannot easily be attributed to a single reaction step of the pump cycle. The kinetics of the falling phase are dominated by the rate-limiting conformational change, $(Na_3)E_1$-P $\rightarrow$ P-$E_2(Na_3)$, the rate of which is in the range of k_{cat} derived from the specific activity of the ATPase (see Materials and Methods) (Heyse et al., 1994). However, even the rate of the falling phase is slower with NPE-caged ATP than with DMB-caged ATP. Only the latter compound can be assumed to generate an instantaneous ATP concentration jump, because its release kinetics are fast compared with the other rate constants involved ($a_f \times [ATP] \approx 100-600\ s^{-1}$, $p_f = 600\ s^{-1}$, $l_f = 25\ s^{-1}$).

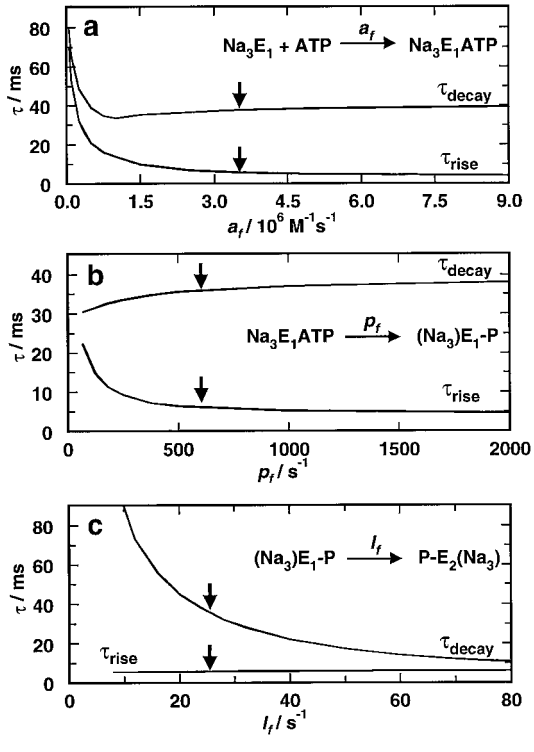

FIGURE 8 Effect of varying the kinetics of selected reaction steps on τ_{rise} and τ_{decay} of transient currents. First numerical simulations were performed in which successively one of a_f, p_f, or l_f was continuously varied, according to Fig. 1 and its mathematical description in the Appendix. The resulting transients were fitted by Eq. 1 to obtain τ_{rise} and τ_{decay}, which are plotted against the varied rate constant. The arrows indicate the value of the pertinent rate constant in Table 1 that was used throughout the rest of this paper. (*a*) $a_f = 3.6 \times 10^6\ M^{-1}\ s^{-1}$; (*b*) $p_f = 600\ s^{-1}$; (*c*) $l_f = 25\ s^{-1}$.

Dependence of the transients on pH

The pH dependence of the kinetics of elementary steps of the Na^+-only mode of the ATPase was clarified when DMB-caged ATP was used instead of NPE-caged ATP (Fig. 5, *a* and *b*). The simulations (*smooth line traces*) in Fig. 5 *a* indicated that the rate constants of the steps that determine the transient currents are virtually independent of pH between pH 6 and pH 8. The rate of the falling phase is predominantly controlled by l_f, and one might expect that phase to be faster at pH 7 than at pH 6 or pH 8, because the specific activity of the enzyme is almost twice as large at pH 7 (Fig. 5 *b*). The deceleration of the transient currents at pH values above 8 can be ascribed only in part to the decrease in the specific activity of the ATPase as pH increases. To illustrate, suppose k_2 decreases from 25 s^{-1} to 12.5 s^{-1} and k_1 is 200 s^{-1}; then t_{max} increases from 11.9 ms to 14.8 ms. The actual increase in t_{max} above pH 8 is larger than is predicted by this calculation, suggesting that the rate constants of steps leading to the formation of $(Na_3)E_1$-P are smaller above pH 8. These complexities in the pH dependence are in line with the report that the rate of the $E_1 \rightarrow$ P-E_2 conformational transition decreases above pH 7.5 (Forbush and Klodos, 1991) and will require further investigation.

ATP concentration dependence

The question of whether the step involving ATP binding to ATPase is associated with the rising or falling phase of the transient current has been controversial (Fendler et al., 1985, 1987, 1993; Borlinghaus and Apell, 1988). Evidence that it is associated with the falling phase comes predominantly from considerations of the effect on the transients of

the slow rate of NPE-caged ATP photolysis and the binding of NPE-caged ATP to the ATP site of the pump. When the experiments were performed with DMB-caged ATP, analysis using Eq. 1 showed that both phases of the current transients were affected by the ATP concentration-dependent reaction step (Fig. 4 *c*), a result consistent with Fig. 1 and rate constant assignments in Table 1.

On photolysis of DMB-caged ATP, t_{max} remained approximately constant (Fig. 4 *b*) and increased only below a released ATP concentration of 20 μM (an estimated 23 μM ATP was released from 0.82 mM DMB-caged ATP at relative light intensity 0.4). The ATP concentration dependence of τ_{rise} behaved similarly and can be explained from the data in Table 1. Thus if a_f is 3.6×10^6 M^{-1} s^{-1} when ATP is <20 μM, the rate constant a_f[ATP] < 72 s^{-1} and becomes comparable to l_f. The equivalent effect is plotted in Fig. 8 *a*. Because in the simulations a_f occurs always as $a_f \times$ [ATP], a variation in a_f by a given factor generates the same response as variation in [ATP] by the same factor with a_f invariant. As can be seen, τ_{rise} increases at low a_f. In our experiments, τ_{rise} and τ_{decay} were also influenced by the ATP concentration, with significant increase at low concentrations (<40 μM ATP released; Fig. 4 *c*), in agreement with the simulations (Fig. 8 *a*). This increase is probably due to a limiting reaction flux through the reaction step $Na_3E_1 + ATP \rightarrow Na_3E_1ATP$ for the transient currents.

Sodium concentration dependence

The kinetics of the transient currents exhibited a complex dependence on the (cytoplasmic) Na^+ concentration (Fig. 6). Numerical simulations of the reaction scheme (Fig. 1) following DMB-caged ATP photolysis reproduced the experiments in a qualitative way by using the parameters of Table 1. The decrease of $1/t_{max}$ below 50 mM Na^+ is caused by the relatively low binding affinity of Na^+ ions for E_1. The decrease of $1/t_{max}$ above 50 mM is also qualitatively reproduced by the simulations, but we do not have a mechanistic explanation for this effect, because t_{max} is a complex function of k_1 and k_2 (Eq. 2) and, subsequently, of ion-binding and release steps. The difference between experimental and calculated values at 400 mM Na^+ may be caused by a decrease in the Na,K-ATPase-specific activity at high ionic strength (Heyse et al., 1994).

The slow photolysis of NPE-caged ATP and its possible binding to the ATP site distorted the pump kinetics (*dashed line* in Fig. 6 *a*; data from Borlinghaus and Apell, 1988). Fig. 6, *b* and *c*, reveal that both time constants, τ_{rise} and τ_{decay}, are functions of the Na^+ concentration, with a reasonable fit between the model and the data obtained using DMB-caged ATP. Whereas τ_{decay} changed by less than a factor of 2 between 2 mM and 150 mM Na^+, τ_{rise} varied 15-fold in the same concentration range. An explanation is the influence of the relatively weak binding for Na^+ with a dissociation constant in the range 5–10 mM for state Na_3E_1, so less Na_3E_1 is available for phosphorylation by ATP.

In principle it would be attractive to analyze I_{max} and the total charge movement as a function of Na^+ concentration, but the variability of the number of adsorbed Na,K-ATPase molecules in the successive experiments rendered such analysis unreliable.

ADP concentration dependence

In analyses of transient currents from experiments with NPE-caged ATP (Borlinghaus et al., 1987; Borlinghaus and Apell, 1988; Wuddel and Apell, 1995), the rate constants controlling $Na_3E_1ATP \rightarrow (Na_3)E_1$-P could not be determined unambiguously because of the slow release kinetics of NPE-caged ATP. The rate constant p_f was therefore estimated to be ≥ 200 s^{-1}, the lower limit being defined by the experiments. Fast release of ATP from DMB-caged ATP circumvents the problem and permits estimates to be made of both p_f and p_b (Fig. 1). Numerical simulations were performed in which p_f and p_b were varied to reproduce the ADP concentration dependence of the transients (Fig. 7); other parameters of Table 1 were kept constant. The solid lines in Fig. 7 were obtained for $p_f = 600$ s^{-1} and $p_b = 1.5 \times 10^6$ M^{-1} s^{-1}. The equilibrium association constant of this reaction is $K_p \equiv p_b/p_f = 2.5 \times 10^3$ M^{-1}. The kinetic parameters showed an almost linear dependence on ADP concentration, and the numerical simulations satisfactorily reproduced the experimental findings (Fig. 7, *b* and *c*). However, the calculated values of $I_{max}/I_{max}(0)$, when based on a half-saturating concentration of 40 μM ($= 1/K_p$), lie above the solid line in Fig. 7 *a*. This discrepancy could be corrected by taking into account the fact that ADP affects another step of the reaction sequence, viz. $Na_3E_1 \rightarrow Na_3E_1ATP$, by competition with ATP binding with a half-saturating concentration of 100 μM ADP (Apell et al., 1986). When this additional effect, which hardly influenced the kinetic parameters of the transient (Fig. 7, *b* and *c*), was included in the simulations, an excellent reproduction of the experimental data could be obtained (*solid line* in Fig. 7 *a*).

This is expected because the combination of ADP interacting with Na_3E_1 and $(Na_3)E_1$-P should lead to a smaller K_i value than $1/K_p$ or the 100 μM K_d for ADP at the ATP binding site. However, although the transient current kinetics are consistent with the model of Wuddel and Apell (1995), they are also compatible with more complex schemes such as that introduced by Keillor and Jencks (1996). Their data showed that phosphorylation of Na_3E_1 could be described by a two-step transformation of the Na_3E_1ATP to $(Na_3)E_1$-P. Although they consider the effect of ADP binding to Na_3E_1 in competition with ATP, as we have done, they do not postulate that this interaction could be an alternative explanation for the two-step phosphorylation.

The data from the ADP-dependent measurements also bear on the electrogenicity of the steps in the Na-only mode of the ATPase. The experiments were performed in the presence of 150 mM NaCl; therefore the cytoplasmic ion sites are occupied before ATP release and the reaction

sequence from Na_3E_1 to P-E_2 (Fig. 1) is valid for these experiments. Only the steps involving Na^+ dissociation from P-E_2, P-$E_2(Na_3) \rightleftharpoons$ P-E_2 contribute to the current because of their positive dielectric coefficients (Table 1). In addition, the major electrogenic step is fast ($g_{3f} = 1400\ s^{-1}$; Wuddel and Apell, 1995) and follows the rate-limiting conformational change, $(Na_3)E_1$-P $\rightleftharpoons$ P-$E_2(Na_3)$, with $l_f = 25\ s^{-1}$.

Because the steps leading to phosphorylation are significantly faster than the conformational change (controlled by a_f, a_b, p_f, and p_b and by l_f, respectively; Table 1), the states Na_3E_1ATP and $(Na_3)E_1$-P will be in an ADP-dependent pseudo-steady state. During this steady-state phase the higher the ADP concentration, the lower the population of state $(Na_3)E_1$-P and so the smaller the observed electric current, because it is controlled mainly by the flux through the rate-limiting step, $\Phi_l = l_f\,[(Na_3)E_1\text{-P}] - l_b\,[\text{P-}E_2(Na_3)]$. Because I_{max} is an approximation for the reaction flux through the rate-limiting step (see Introduction), the data of Fig. 7 *a* support this interpretation.

An alternative model of the Na^+ translocation has been discussed by Fendler et al. (1987, 1993), who proposed that enzyme phosphorylation is rate-limiting and is followed by a fast conformational change. In the absence of ADP, a sequence of a fast and a slow reaction step cannot be discriminated from the reverse order sequence, because the current signals are produced from subsequent ion release steps. However, the ADP concentration dependence of the first step allows an insight into the order. If in numerical simulations the values of p_f and l_f are exchanged and the equilibrium constants K_p and K_f are kept constant, the current transients at [ADP] = 0 are equal, as expected. With increasing ADP concentrations, the reduction in I_{max} is significantly less pronounced (Fig. 7 *a*, *dashed line*) than found experimentally, and if the competitive binding of ADP to state Na_3E_1 is abolished, I_{max} is found to be virtually concentration independent up to 300 μM ADP (not shown). A mechanistic explanation for this finding is the low population of state $(Na_3)E_1$-P, which is always drained by the fast conformational change. Hence only extremely high ADP concentrations would affect the reaction flux. The experimentally determined ADP concentration dependence of I_{max} is therefore evidence in favor of a model in which the ADP-dependent reaction is followed by a rate-limiting step.

CONCLUSIONS

The major advantage of the use of DMB-caged ATP in electrical measurements with Na,K-ATPase in purified membrane fragments is that the release rate from the caged precursor is faster than rates of the protein kinetics over all pH values. We have confirmed that the relatively slow photolysis of NPE-caged ATP affects the shape of transient currents triggered by photolytic release of ATP, and have shown that the much faster ATP release from DMB-caged ATP allows more direct analysis of the transients in terms of the Na-only mode of the Na,K-ATPase. ATP association and enzyme phosphorylation affect both the rising and falling phases of the transient current, whereas the rate-limiting $(Na_3)E_1$-P to P-$E_2(Na_3)$ conformational change dominates the kinetics of the falling phase. Rate constants of ATP association, a_f ($= 3.5 \times 10^6\ M^{-1}\ s^{-1}$), and of the rate-limiting conformational change, l_f ($= 25\ s^{-1}$), are consistent with earlier estimates. The rate constant of enzyme phosphorylation, p_f ($= 600\ s^{-1}$), needs correction from the value of 200 s^{-1} previously assigned (Mårdh and Zetterquist, 1974; Heyse et al., 1994). Experiments in the presence of various concentrations of ADP permit evaluation of the rate constant of the ADP-dependent dephosphorylation, p_b ($= 1.5 \times 10^6\ M^{-1}\ s^{-1}$). The influence of Na^+ concentration and pH on the transients is broadly consistent with earlier studies (Heyse et al., 1994; Wuddel and Apell, 1995) and with the pH dependence of the specific activity of Na,K-ATPase.

APPENDIX: NUMERICAL ANALYSIS OF THE TRANSIENT PUMP CURRENT

To simulate current transients mediated by the ion pump, a detailed mathematical model was formulated on the basis of the reaction scheme of Fig. 1 (Wuddel and Apell, 1995). In a FORTRAN program, a system of 10 coupled differential equations as a formalized representation of the pump cycle in Fig. 1 were solved with rate constants and dielectric coefficients listed in Table 1 and with appropriate boundary conditions corresponding to the experimental conditions of the respective experiments. The principal difference from the model is that release of ATP from DMB-caged ATP is much faster than any other rate constant in the reaction sequence $E_1 \rightarrow \ldots \rightarrow$ P-E_2 and therefore is assumed to occur instantaneously at the time of the light flash. Therefore we introduced

$$c_T(t) \equiv [\text{ATP}] = \vartheta[\text{DMB-caged ATP}]\exp(-t/\tau_a) \quad \text{for } t > 0$$

and

$$c_T(t) = 0 \quad \text{for } t \leq 0.$$

ϑ is the yield of ATP released from DMB-caged ATP, and the value of 3 s for τ_a is an empirically determined constant, which depends on diffusion of ATP out of the vicinity of the membrane and on ATP hydrolysis by apyrase and Na,K-ATPase (Wuddel and Apell, 1995).

Experiments with NPE-caged ATP were analyzed as presented by Wuddel and Apell (1995), with

$$c_T(t) \equiv [\text{ATP}] = \vartheta[\text{NPE-caged ATP}]\{1 - \exp(-\lambda t)\}\exp(-t/\tau_a)$$

$$\lambda = 8.6 \times 10^8 \times 10^{-\text{pH}}\ s^{-1},$$

where λ describes the pH-dependent kinetics of the photolysis of NPE-caged ATP (Borlinghaus and Apell, 1988; Walker et al., 1988).

The rate constants and dielectric coefficients used in the simulations as presented in Figs. 2, 5*a*, and 6–8 are given in Table 1.

Note added in proof: Recently Kane et al. (1997, *Biochemistry* 36:13406–13420) reported a rate of the phosphorylation reaction measured by stopped flow and quenched-flow techniques of 190 s^{-1} and suggested a very fast conformational change ($\geq$ 600 S^{-1}).

We are grateful to Milena Roudna for excellent technical assistance, to Gordon Reid for synthesis of DMB-caged ATP, and to Dr. Ingo Wuddel for helpful discussions.

This work was supported by the Deutsche Forschungsgemeinschaft (Sonderforschungsbereich 156).

REFERENCES

Apell, H.-J., R. Borlinghaus, and P. Läuger. 1987. Fast charge transitions associated with partial reactions of the Na,K pump. II. Microscopic analysis of transient currents. *J. Membr. Biol.* 97:179–181.

Apell, H.-J., and M. M. Marcus. 1986. (Na^+,K^+)-ATPase in artificial lipid vesicles: influence of the concentration of mono- and divalent cations on the pumping rate. *Biochim. Biophys. Acta.* 862:254–264.

Apell, H.-J., M. T. Nelson, M. M. Marcus, and P. Läuger. 1986. Effects of the ATP, ADP and inorganic phosphate on the transport rate of the Na^+,K^+ pump. *Biochim. Biophys. Acta.* 857:105–115.

Apell, H.-J., M. Roudna, J. E. T. Corrie, and D. R. Trentham. 1996. Kinetics of the phosphorylation of Na,K-ATPase by inorganic phosphate detected by a fluorescence method. *Biochemistry.* 35:10922–10930.

Borlinghaus, R., and H.-J. Apell. 1988. Current transients generated by the Na^+/K^+-ATPase after an ATP concentration jump: dependence on sodium and ATP concentration. *Biochim. Biophys. Acta.* 939:197–206.

Borlinghaus, R., H.-J. Apell, and Läuger, P. 1987. Fast charge translocations associated with partial reactions of the Na,K pump. I. Current and voltage transients after photochemical release of ATP. *J. Membr. Biol.* 97:161–178.

Bühler, R., W. Stürmer, H.-J. Apell, and P. Läuger. 1991. Charge translocation by the Na,K pump. I. Kinetics of local field changes studied by time-resolved fluorescence measurements. *J. Membr. Biol.* 121: 141–161.

Corrie, J. E. T., Y. Katayama, G. P. Reid, M. Anson, and D. R. Trentham. 1992. The development and application of photosensitive caged compounds to aid time-resolved structure determinations of macromolecules. *Philos. Trans. R. Soc. Lond. A.* 340:233–244.

Fendler, K., E. Grell, and E. Bamberg. 1987. Kinetics of pump currents generated by the Na^+, K^+ ATPase from kidney on black lipid membranes. *FEBS Lett.* 224:83–88.

Fendler, K., E. Grell, M. Haubs, and E. Bamberg. 1985. Pump currents generated by the purified Na^+,K^+-ATPase from kidney on black lipid membranes. *EMBO J.* 4:3079–3085.

Fendler, K., S. Jaruschewski, A. S. Hobbs, W. Albers, and J. P. Froehlich. 1993. Pre-steady-state charge translocation in Na,K-ATPase from eel electric organ. *J. Gen. Physiol.* 102:631–666.

Forbush, B. 1984a. Na^+ movement in a single turnover of the Na pump. *Proc. Natl. Acad. Sci. USA.* 81:5310–5314.

Forbush, B., 1984b. An apparatus for rapid kinetic analysis of isotopic efflux from membrane vesicles and of ligand dissociation from membrane proteins. *Anal. Biochem.* 140:495–505.

Forbush, B., and I. Klodos. 1991. Rate-limiting steps in Na^+ translocation by the Na/K Pump. *In* The Sodium Pump. Structure, Mechanism, and Regulation. J. H. Kaplan and P. De Weer, editors. Rockefeller University Press, New York. 211–225.

Friedrich, T., E. Bamberg, and G. Nagel. 1996. Na^+,K^+-ATPase pump currents in giant excised patches activated by an ATP concentration jump. *Biophys. J.* 71:2486–2500.

Friedrich, T., and G. Nagel. 1997. Comparison of Na^+/K^+-ATPase pump currents activated by ATP concentration or voltage jumps. *Biophys. J.* 73:186–194.

Gadsby, D. C., M. Nakao, and A. Bahinski. 1991. Voltage-induced Na/K pump charge movements in dialyzed heart cells. *In* The Sodium Pump: Structure, Mechanism and Regulation. J. H. Kaplan and P. De Weer, editors. Rockefeller University Press, New York. 355–371.

Gadsby, D. C., R. F. Rakowski, and P. De Weer. 1993. Extracellular access to the Na,K pump: pathway similar to ion channel. *Science.* 260: 100–103.

Glynn, I. M. 1985. The Na^+,K^+-transporting adenosine triphosphatase. *In* The Enzymes of Biological Membranes, Vol. 3, 2nd Ed. A. N. Martonosi, editor. Plenum, New York. 35–114.

Heyse, S., I. Wuddel, H.-J. Apell, and W. Stürmer. 1994. Partial reactions of the Na,K-ATPase: determination of rate constants. *J. Gen. Physiol.* 104:197–240.

Hilgemann, D. W. 1994. Channel-like function of the Na,K pump probed at microsecond resolution in giant membrane patches. *Science.* 263: 1429–1432.

Jørgensen, P. L. 1974. Isolation of the (Na^+ + K^+)-ATPase. *Methods Enzymol.* 32:277–290.

Keillor, J. W., and W. P. Jencks. 1996. Phosphorylation of the sodium-potassium adenosinetriphosphatase proceeds through a rate-limiting conformational change followed by rapid phosphoryl transfer. *Biochemistry.* 35:2750–2753.

Klodos, I., and B. Forbush. 1988. Rapid conformational changes of the Na/K pump revealed by a fluorescent dye RH-160. *J. Gen. Physiol.* 92:46a.

Läuger, P. 1991. Electrogenic Ion Pumps. Sinauer Associates, Sunderland, MA.

Läuger, P., and H.-J. Apell. 1986. A microscopic model for the current-voltage behaviour of the Na,K-pump. *Eur. Biophys. J.* 13:309–321.

Lowry, O. H., N. J. Rosebrough, A. L. Farr, and R. J. Randall. 1951. Protein measurement with the Folin phenol reagent. *J. Biol. Chem.* 193:265–275.

Lu, C.-C., A. Kabakov, V. S. Markin, S. Mager, G. A. Frazier, and D. W. Hilgemann. 1995. Membrane transport mechanisms probed with megahertz voltage clamp. *Proc. Natl. Acad. Sci. USA.* 92:11220–11224.

Mårdh, S., and Ö. Zetterquist. 1974. Phosphorylation from adenosine triphosphate of sodium- and potassium-activated adenosine triphosphatase. *J. Biol. Chem.* 252:633–638.

McCray, J. A., and D. R. Trentham. 1989. Properties and uses of photoreactive caged compounds. *Annu. Rev. Biophys. Biophys. Chem.* 18: 239–270.

Nagel, G., K. Fendler, E. Grell, and E. Bamberg. 1987. Na^+ currents generated by the purified (Na^+ and K^+)-ATPase on planar lipid membranes. *Biochim. Biophys. Acta.* 901:239–249.

Nakao, M., and D. C. Gadsby. 1986. Voltage dependence of Na^+ translocation by the Na/K pump. *Nature.* 323:628–630.

Nakao, M., and D. C. Gadsby. 1989. [Na^+] and [K^+] dependence of the Na/K pump current-voltage relationship in guinea pig ventricular myocytes. *J. Gen. Physiol.* 94:539–565.

Rakowski, R. F., L. A. Vasilets, J. La Tona, and W. Schwarz. 1991. A negative slope in the current-voltage relationship of the Na^+/K^+ pump in *Xenopus* oocytes produced by reduction of external [K^+]. *J. Membr. Biol.* 121:171–187.

Sagar, A., and R. F. Rakowski. 1994. Access channel model for the voltage dependence of the forward-running Na^+/K^+ pump. *J. Gen. Physiol.* 103:869–894.

Schulz, S., and H.-J. Apell. 1995. Investigation of ion binding to the cytoplasmic binding sites of the Na,K-pump. *Eur. Biophys. J.* 23: 413–421.

Schwartz, A., K. Nagano, M. Nakao, G. E. Lindenmayer, and J. C. Allen. 1971. The sodium- and potassium-activated adenosine triphosphatase system. *Methods Pharmacol.* 1:361–388.

Sheehan, J. C., R. M. Wilson, and A. W. Oxford. 1971. The photolysis of methoxy-substituted benzoin esters. A photosensitive protecting group for carboxylic acids. *J. Am. Chem. Soc.* 93:7222–7278.

Sokolov, V. S., H.-J. Apell, J. E. T. Corrie, and D. R. Trentham. 1997. Fast transient currents in the Na,K-ATPase induced by ATP concentration jump experiments from DMB-caged ATP. *Biophys. J.* 72:A291.

Stürmer, W., R. Bühler, H.-J. Apell, and P. Läuger. 1991. Charge translocation by the Na,K-pump: ion binding and release studied by time-resolved fluorescence measurements. *In* The Sodium Pump. Recent Developments. J. H. Kaplan and P. De Weer, editors. Rockefeller University Press, New York. 531–536.

Thirlwell, H., J. E. T. Corrie, G. P. Reid, D. R. Trentham, and M. A. Ferenczi. 1994. Kinetics of relaxation from rigor of permeabilized fast-twitch skeletal fibers from the rabbit using a novel caged ATP and apyrase. *Biophys. J.* 67:2436–2447.

Thirlwell, H., J. A. Sleep, and M. A. Ferenczi. 1995. Inhibition of unloaded shortening velocity in permeabilized muscle fibres by caged ATP compounds. *J. Muscle Res. Cell Motil.* 16:131–137.

Vasilets, L. A., H. S. Omay, T. Otha, S. Noguchi, M. Kawamura, and W. Schwarz. 1991. Stimulation of the Na^+/K^+ pump by external $[K^+]$ is regulated by voltage-dependent gating. *J. Biol. Chem.* 266: 16285–16288.

Walker, J. W., G. P. Reid, J. A. McCray, and D. R. Trentham. 1988. Photolabile 1-(2-nitrophenyl)ethyl phosphate esters of adenine nucleotide analogues. Synthesis and mechanism of photolysis. *J. Am. Chem. Soc.* 110:7170–7177.

Wuddel, I. 1994. Untersuchung kinetischer und dielektrischer Eigenschaften der Na,K-ATPase: Hemmstoff und Ladungspuls-Experimente. Dissertation, University of Konstanz. 1–126.

Wuddel, I., and H.-J. Apell, 1995. Electrogenicity of the sodium transport pathway in the Na,K-ATPase probed by charge-pulse experiments. *Biophys. J.* 69:909–921.